(42) Devaux, J.; Godard, P.; Mercier, J. P.; Touillaux, R.; Dereppe, J. M. J. Polym. Sci., Polym. Phys. Ed. 1982, 20, 1881.
(43) Devaux, J.; Godard, P.; Mercier, J. P. J. Polym. Sci., Polym. Phys. Ed. 1982, 20, 1895.
(44) Devaux, J.; Godard, P.; Mercier, J. P. J. Polym. Sci., Polym. Phys. Ed. 1982, 20, 1901.
(45) Pilati, F.; Marianucci, E.; Berti, C. J. Appl. Polym. Sci. 1985, 30, 1267.

# Evaluation of the Lattice Strain Energy Density in Polyethylene Crystals

**Hervé Marand***

*Michigan Molecular Institute, 1910 W. St. Andrews Road, Midland, Michigan 48640.*
*Received November 16, 1988; Revised Manuscript Received March 24, 1989*

ABSTRACT: Molecular energy calculations are used to assess the lattice strain energy density $\epsilon$ and the corresponding interfacial surface free energy $\sigma_s$ in melt-crystallized polyethylene crystals. The quantity $\epsilon$, which is defined as the difference in lattice energy density between an unstrained crystal and a strained crystal, is calculated with the use of published lattice expansion data. A strain-induced interfacial surface free energy $\sigma_s$ of about 0.9 erg·cm$^{-2}$ (mJ·m$^{-2}$) was derived from the strain energy density for a lamellar thickness of around 14 nm. This result compares favorably with the value obtained in the recent extension of nucleation theory by Hoffman and Miller describing the geometry and the growth kinetics of curved-edge polyethylene crystals.

## Introduction

The goal of this paper is to provide by a direct method the value of the lattice strain energy density, which according to a recent treatment by Hoffman and Miller (HM) is at the origin of the existence of curved-edge polyethylene crystals. Hoffman and Miller proposed a generalization of the nucleation theory to account for the origin and growth kinetics of chain-folded polymer crystals with curved edges.[1] Their treatment is based on the existence of lattice strain in (200) sectors and on a detailed description of the nucleation and growth characteristics for both the (110) and the (200) sectors making the curved-edge crystal. The growth in the (110) sectors can be accounted for by standard nucleation theory,[2] where the growth front is represented by a flat surface. The growth front of the (200) sector, on the other hand, is described in the extended theory by a "serrated surface". The concomitant effect of such a serrated surface and of the lattice strain allows one to account for (1) the growth rate data obtained by Organ and Keller,[3] (2) the values of the of axial ratio and ellipticity of these curved-edge crystals,[4] and (3) the observation of different melting points for (110) and (200) sectors.[5] The agreement between theory and experiments rests, however, on the physical soundness of the value obtained for the single fitting parameter in the HM treatment, i.e., the strain-induced interfacial surface free energy $\sigma_s$, which we will calculate from the lattice strain energy density $\epsilon$ (cf. later). The parameter $\sigma_s$ is involved in the kinetics of the substrate completion rate and in the expression for the reduced melting point exhibited by the (200) sectors.

The existence of lattice strain was demonstrated in the work of Davis et al.,[6] where the unit cell dimensions $a$ and $b$ of polyethylene crystals were measured by X-ray diffraction as a function of lamellar thickness. The steady increase of $a$ and $b$ dimensions with the reciprocal of lamellar thickness suggested that the lattice expansion arises from the repulsion between neighboring folds on the crystal surface. Upon careful examination of their data, it is apparent in the case of melt-crystallized polyethylene that the expansion is mainly between the (200) planes (i.e., between the (200) folds). This is consistent with the experimental observation by Bassett et al.[7] that the (200) sectors in melt-crystallized polyethylene single crystals are growth inhibited (using the concepts developed by Hoffman and Miller for the case of crystals grown from solution at low undercooling). It is also consistent with the observation of a $b$ axis radial orientation in polyethylene spherulites. The $b$ axis radial orientation arises from the faster growth of the (110) front as compared to the (200) (the latter is slowed down as a result of the strain between (200) planes). It can be suggested that although the growth occurs faster along the $b$ axis, a large number of the folds will be of the (200) type, since (200) sectors occupy a much larger volume than the (110) (Figure 1). Such an hypothesis is consistent with the results of a recent study by Wittmann and Lotz.[8] Using the polymer decoration technique, they found that a large fraction of the lamellar structure had to result from lateral growth. This does not contradict the general idea that the crystallization process is kinetically controlled by nucleation on the (110) growth front. Further evidence of the repulsion between (200) planes can also be found in the recent work of Davé and Farmer,[9] where by molecular energy calculations they showed that, because of their bulkiness, (200) folds strongly repel each other.

We propose, here, to calculate the lattice strain energy density in polyethylene crystals by the technique of molecular mechanics, using the experimentally measured unit cell dimensions of Davis et al.[6]

**Table I**
**Nonbonded Potential Parameters for C•••C, C•••H, and H•••H[a]**

| | $A$ | $B$ | $C$ |
|---|---|---|---|
| C···C | −2.452 | 363 631 | 36.0 |
| C···H | −0.468 | 32 970 | 36.7 |
| H···H | −0.140 | 12 230 | 37.4 |

[a] $A$, $B$, and $C$ are given respectively in J·nm$^6$·mol$^{-1}$, kJ·mol$^{-1}$, and nm$^{-1}$ (from ref 14).

## Molecular Mechanics

Molecular mechanics has proven very valuable in predicting the packing and structure of molecular crystals,[10,11] in providing possible mechanisms for crystal–crystal transitions,[12] in examining the energetics of chain folding,[9]

* Permanent address: Virginia Polytechnic Institute and State University, Chemistry Department, Blacksburg, Virginia 24061.

0024-9297/89/2222-3980$01.50/0 

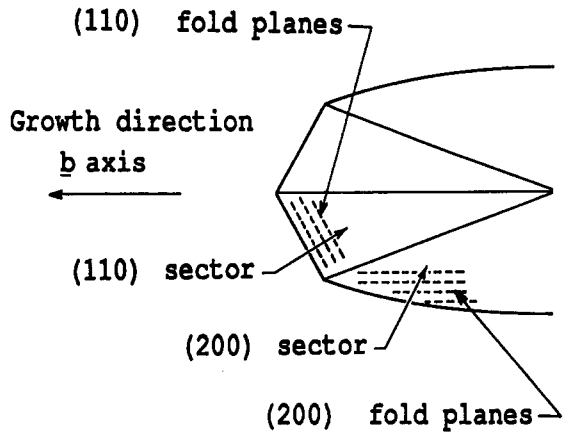


**Figure 1.** Schematic of a curved-edge polyethylene crystal exhibiting (110) and (200) growth fronts and fold planes.

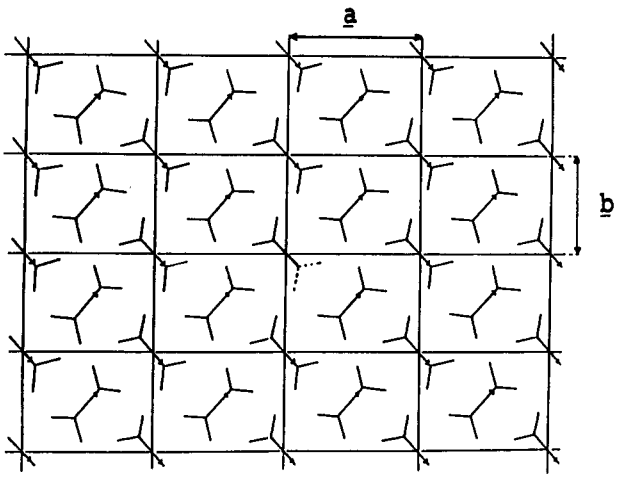


**Figure 2.** Projection in the $a$, $b$ plane of the orthorhombic polyethylene lattice: the dotted lines at the center of the lattice correspond to the reference $CH_2$.

and even in estimating activation energies for self-diffusion in paraffin crystals.[13] The present method is based on the use of the empirical nonbonded atomic potentials obtained by Williams[14] by fitting of experimental data on hydrocarbons. The nonbonded potentials at distances $\mathbf{r}$ between atoms in different stems are of the exp–6 type:

$$\Phi(\mathbf{r}) = A^*\mathbf{r}^{-6} + B^* \exp(-C^*\mathbf{r}) \quad (1)$$

where the constants $A$, $B$, and $C$ for the C···C, C···H, and H···H interactions are listed in Table I. The lattice energy is then calculated by pairwise summation of the atom–atom interactions over an orthorhombic polyethylene lattice of sufficiently large size to avoid truncation effects:

$$E_l = (1/2)\sum_i \Phi'((CH_2)^0,(CH_2)^i) \quad (2)$$

where $\Phi'$ is the interaction energy between the reference $CH_2$ at the center of the lattice (superscript 0) and a $CH_2$ at any position in the lattice (superscript $i$) (Figure 2). $\Phi'$ is then expressed in terms of the nine atomic potentials $\Phi(C^0\cdots C^i)$, $\Phi(C^0\cdots H1^i)$, $\Phi(C^0\cdots H2^i)$, $\Phi(H1^0\cdots C^i)$, $\Phi(H1^0\cdots H1^i)$, etc... The atomic positions in the lattice are defined in terms of the unit cell dimensions $a$, $b$, and $c$, the setting angle $\theta$, the C–C and C–H bond lengths, and the C–C–C and H–C–H bond angles.

The first step in these calculations consists in finding the $a$ and $b$ cell dimensions corresponding to the minimum lattice energy, taking for granted that the other parameters ($c$, bond lengths, bond angles, and setting angle) are already known (Table II). Varying $a$ and $b$ by $5 \times 10^{-4}$ nm increments between 0.7 and 0.75 nm and 0.47 and 0.52 nm,

**Table II**
**Molecular Characteristics of Paraffin Chain Crystals (from Dave and Farmer[9])**

| | | | |
|---|---|---|---|
| C–C bond length | 0.1534 nm | C–C–C bond angle | 112.0° |
| C–H bond length | 0.1090 nm | H–C–H bond angle | 109.4° |
| $c$ | 0.254 nm | setting angle | 48.0° |

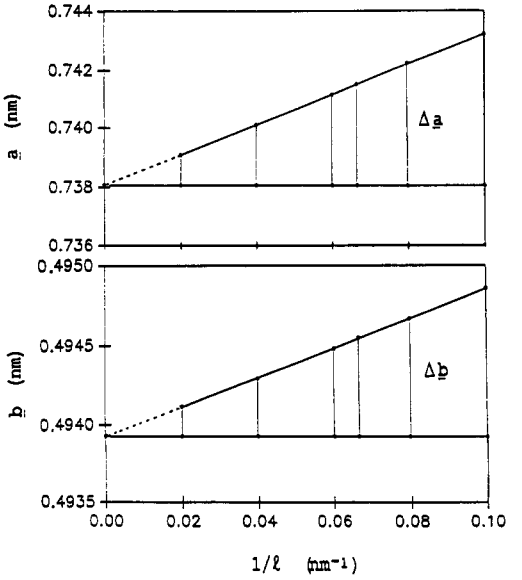


**Figure 3.** $a$ and $b$ unit cell expansion and corresponding lattice strain, $\Delta a$ and $\Delta b$, as a function of reciprocal lamellar thickness $1/l$ (from the data set $M_1$ of Davis et al.[6] recorded at 296.2 K).

respectively, resulted in a minimum lattice energy of –8.16 kJ/mol ($CH_2$) for $a = 0.710$ nm and $b = 0.4905$ nm, for a cutoff distance of 2 nm in the summation (this corresponds to over 99% of the total interaction energy in an infinite lattice). This value is in good agreement with the results of Yemni and McCullough[12] and with the value of the heat of sublimation at 0 K derived from thermodynamic data on $n$-paraffins by Billmeyer ($E_l = -7.70$ kJ/mol ($CH_2$)).[15] We must, however, keep in mind that the values calculated for the lattice energy and the lattice cell dimensions are truly representative of the crystal at a temperature around 150 K where the Williams potential parameters were determined. Making use of the paraffin heat capacity data between 0 and 150 K, one can calculate the heat of sublimation at 150 K and bring the experimentally backed-up value of the lattice energy in closer agreement with the value calculated here. Along the same lines, the relatively low values obtained for $a$ and $b$ arise from the fact that they are calculated at low temperature and thus do not account for thermal expansion, and they correspond to infinitely long paraffin chains that are not affected by the presence of folds. To account for the presence of folds and their effect on cell expansion, one can first extrapolate the data of Davis et al.[6] (Figure 3) to infinite lamellar thickness, where the influence of the folds is minimum, and then calculate the relative expansion in both $a$ and $b$ directions corresponding to a given lamellar thickness. The calculated relative expansions $\Delta a$ and $\Delta b$ are then used in the calculation of the lattice energy. The lattice strain energy density $\epsilon$ is obtained as the difference in lattice energy between unstrained crystal $E^u_l$ ($a^u = 0.710$ nm, $b^u = 0.4905$ nm) and the strained crystal $E^s_l$ ($a = a^u + \Delta a$, $b = b^u + \Delta b$):

$$\epsilon\ (\mathrm{J/cm^3}) = -\frac{4}{cN_a}\left(\frac{E^u_l}{a^u b^u} - \frac{E^s_l}{ab}\right) \quad (3)$$

where $N_a$ is the Avogadro number. In eq 3, the presence

**Table III**
**Lattice Energy, Strain Energy Density, and Strain-Induced Interfacial Surface Free Energy as a Function of Lattice Strain[a]**

| $l$ | $10^3\Delta a$ | $10^3\Delta b$ | $a$ | $b$ | $E^u_l$ | $\epsilon$ | $\sigma_s$ |
|---|---|---|---|---|---|---|---|
| $\infty$ | 0.! | 0.! | 0.7100 | 0.4905 | −8.1704 | 0.0 | 0.0 |
| 50.0 | 1.1 | 0.2 | 0.7111 | 0.4907 | −8.1702 | 1.21 | 0.25 |
| 25.0 | 1.1 | 0.4 | 0.7122 | 0.4909 | −8.1694 | 2.47 | 0.50 |
| 15.0 | 3.6 | 0.6 | 0.7136 | 0.4911 | −8.1673 | 4.18 | 0.85 |
| 12.5 | 4.3 | 0.8 | 0.7143 | 0.4913 | −8.1660 | 5.02 | 1.02 |
| 10.0 | 5.3 | 1.0 | 0.7153 | 0.4915 | −8.1636 | 6.28 | 1.27 |

[a] $l$, $\Delta a$, $\Delta b$, $a$, and $b$ are in nm, $E^u_l$ in kJ/mol ($CH_2$), $\epsilon$ in J/cm$^3$, and $\sigma_s$ in erg·cm$^{-2}$ (1 erg·cm$^{-2}$ = 1 mJ·m$^{-2}$); ! corresponds to the minimum lattice energy ($a^u$, $b^u$, and $E^u_l$).

of $a^u b^u$ and $ab$ is required to transform the molar energy into energy density. The results of these calculations for various sets of $a$, $b$, and $l$ from Figure 3 are listed in Table III.

## Discussion

Although it was noticed in the HM treatment that the expansion is mainly along the $a$ axis, the lattice strain energy density was modeled by an interfacial surface free energy that is isotropic in the $a$, $b$ plane. It is certainly as valid an approximation as the one that describes the lateral surface free energy in terms of a single parameter $\sigma$. With this in mind, the chain will occupy a volume $a_0 b_0 l$ on the (200) growth front, where $l$ is the lamellar thickness and $a_0$ and $b_0$ are defined by

$$a_0 = a \qquad b_0 = b/2$$

The interfacial surface free energy $\sigma_s$ employed by HM is then obtained by

$$2[(a_0/2)^2 + b_0^2]^{1/2} l \sigma_s = a_0 b_0 l \epsilon \tag{4}$$

which can be rearranged as

$$\sigma_s = \frac{ab}{2[a^2 + b^2]^{1/2}} \epsilon$$

to give the values in the last column of Table III. For the crystallization conditions investigated in ref 1, the lamellar thickness is of the order of 14 ± 2 nm as measured by Raman scattering. Using the results from Table III, one can infer that the corresponding values for $\sigma_s$ are in the range 0.9 ± 0.2 erg·cm$^{-2}$. This is to be compared with the value 1.2 erg·cm$^{-2}$ obtained by Miller and Hoffman[4] for polyethylene single crystals formed in $n$-hexadecane, strictly from considerations based on crystallization kinetics, curvature, and aspect ratio data. It should be pointed out that this calculated value of $\sigma_s$ is truly comparable to the kinetic value of $\sigma_s$ derived by Miller et al., because no thickening takes place during solution crystallization of PE.

Some comment on the validity of this comparison is, however, in order. First, one should observe that the $\sigma_s$ values calculated here correspond to melt-crystallized PE, whereas the one reported by Miller and Hoffman[4] is derived for the case of solution-grown PE crystals. Viewed in this light, the agreement may be regarded as quite satisfactory. It would have been better, a priori, to compare the latter value with the strain-induced interfacial free energy calculated from the data of Davis et al.[6] obtained on single crystals grown from a xylene solution. However, the crystals grown in xylene in the temperature range investigated by Davis and co-workers do not exhibit curved edges, so that $\sigma_s$ cannot be determined by the method described by HM. The $a$ and $b$ unit cell dimensions for these diamond-shaped single crystals are, however, slightly larger than these obtained for paraffin crystals, suggesting that the chain-folded crystals do exhibit a modest level of lattice expansion when compared to the paraffin crystals. This expansion may arise in this case from a slight repulsion between (110) folds. Second, since the tilt of the chain axis with respect to the lamellar normal was not measured for the particular solution-grown crystals under consideration, it is hard to know what the exact value of the lamellar thickness really is. In addition, in contrast with the melt-crystallized PE case, the lamellar thickness dependence of the lattice expansion for solution-grown PE crystals varies with the temperature at which the X-ray data were recorded. For these reasons, it was decided not to attempt to make estimates of $\sigma_s$ by molecular energy calculations for solution-grown crystals.

## Conclusion

We have derived by a direct method an estimate of the lattice strain energy density existing in melt-crystallized PE and thence a value of the corresponding strain-induced interfacial surface free energy $\sigma_s$. The fact that the crystal expansion is primarily along the $a$ axis and is approximately inversely proportional to the lamellar thickness suggests that the principal lattice strain arises from repulsion between (200) folds. Finally, the value derived for the lattice strain energy density and the corresponding $\sigma_s$ in melt-crystallized PE are consistent with the results of the Hoffman–Miller treatment of the kinetics of growth of curved-edge crystals and support the soundness of their model.

**Acknowledgment.** I am grateful to Dr. J. D. Hoffman and Dr. R. L. Miller, both of the Michigan Molecular Institute, for a number of helpful discussions and for providing a copy of their manuscript prior to publication. I also wish to express my appreciation to Dr. R. S. Davé of the Michigan Molecular Institute for his stimulating interaction.

**Registry No.** Polyethylene, 9002-88-4.

## References and Notes

(1) Hoffman, J. D., Miller, R. L. *Macromolecules*, in press.
(2) Hoffman, J. D.; Miller, R. L. *Macromolecules* **1988**, *21*, 3038.
(3) Organ, S. J.; Keller, A. *J. Polym. Sci., Polym. Phys. Ed.* **1986**, *24*, 2319.
(4) Miller, R. L.; Hoffman, J. D., to be submitted for publication in *Polymer*.
(5) (a) Bassett, D. C.; Frank, F. C.; Keller, A. *Nature* **1959**, *184*, 810. (b) Harrison, I. R. *J. Polym. Sci., Polym. Phys. Ed.* **1973**, *11*, 991.
(6) Davis, G. T.; Weeks, J. J.; Martin, G. M.; Eby, R. K. *J. Appl. Phys.* **1974**, *45*, 4175.
(7) Bassett, D. C.; Olley, R. H.; Al Raheil, I. A. M. *Polymer* **1988**, *29*, 1539.
(8) Wittmann, J. C.; Lotz, B. *J. Polym. Sci., Polym. Phys. Ed.* **1985**, *23*, 205.
(9) Davé, R. S.; Farmer, B. L. *Polymer* **1988**, *29*, 1544.
(10) Kitaigorodsky, A. I. In *Molecular Crystals and Molecules*; Academic Press: New York, 1973.
(11) Sorensen, R. A.; Liau, W. B.; Boyd, R. H. *Macromolecules* **1988**, *21*, 194.
(12) Yemni, T.; McCullough, R. L. *J. Polym. Sci., Polym. Phys. Ed.* **1973**, *11*, 1385.
(13) Farmer, B. L.; Eby, R. K. *Polymer* **1987**, *28*, 86.
(14) Williams, D. E. *J. Chem. Phys.* **1967**, *47*, 4680.
(15) Billmeyer, F. W. *J. Appl. Phys.* **1959**, *28*, 1114.